

EIT: ENHANCED INTERACTIVE TRANSFORMER

Tong Zheng^{1†*}, Bei Li^{1*}, Huiwen Bao^{2†*}, Tong Xiao^{1,2‡}, Jingbo Zhu^{1,2}

¹ School of Computer Science and Engineering, Northeastern University, Shenyang, China

² NiuTrans Research, Shenyang, China

{zhengtong12356, goodbaohuiwen}@gmail.com, libei_neu@outlook.com,
{xiaotong, zhujingbo}@mail.neu.edu.cn

ABSTRACT

In this paper, we propose a novel architecture, the Enhanced Interactive Transformer (EIT), to address the issue of head degradation in self-attention mechanisms. Our approach replaces the traditional multi-head self-attention mechanism with the Enhanced Multi-Head Attention (EMHA) mechanism, which relaxes the one-to-one mapping constraint among queries and keys, allowing each query to attend to multiple keys. Furthermore, we introduce two interaction models, Inner-Subspace Interaction and Cross-Subspace Interaction, to fully utilize the many-to-many mapping capabilities of EMHA. Extensive experiments on a wide range of tasks (e.g. machine translation, abstractive summarization, grammar correction, language modelling and brain disease automatic diagnosis) show its superiority with a very modest increase in model size.

1 INTRODUCTION

Transformer (Vaswani et al., 2017) have yielded promising results on a wide range of natural language processing tasks (Devlin et al., 2019; Brown et al., 2020). One of the primary reasons for this success is the multi-head self-attention network (MHSA), which allows the model to capture global dependencies within a sequence by dividing the hidden representation into multiple feature subspaces and performing attention operations within each subspace.

Researchers have found that different heads within the MHSA can capture distinct information, and further regularization through the enlargement of head distance can yield better results (Li et al., 2018). However, it has also been observed that there is redundancy among heads, and pruning some of these heads can be done without affecting performance (Michel et al., 2019). Efforts have been made to more efficiently prune heads (Voita et al., 2019; Behnke & Heafield, 2020), as it has been shown that the vanilla Transformer does not necessarily benefit from more heads on the WMT’14 En-De task. In fact, Figure 1 demonstrates that the performance of the vanilla Transformer on the WMT’14 En-De task significantly deteriorates when the number of heads exceeds 64. As a result, the design of the MHSA is typically limited to a low number of heads, such as 8 or 16 heads for machine translation tasks.

The present study observes two interesting phenomena in regards to the use of Transformer models: first, as noted by Voita et al. (2019), a Transformer model with a lower number of heads may exhibit lower performance compared to a Transformer model with 8 heads that has been pruned to a similar number of heads. Second, as demonstrated by Wang et al. (2022), the addition of more heads can potentially mitigate the occurrence of over-smoothing, a phenomenon in which the representations of different tokens become highly similar and degrade the expressiveness of the model, particularly in the case of deep models. These findings suggest that, both empirically and theoretically, an increase

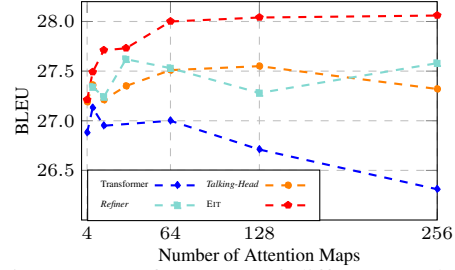


Figure 1: Performance of different models (pre-norm) across the number of attention maps on the WMT’14 En-De task.

*Equal contribution. [†]Research assistant (intern) at NEU. [‡]Corresponding author

in the number of heads may be a practical means of enhancing the expressiveness of Transformer models. Consequently, the question arises: “Can the addition of more heads effectively improve the expressiveness of Transformer models?”

We first investigate the difficulties of benefiting from more heads in Transformer. Recently, Shazeer et al. (2020) argue that too many heads cannot guarantee precise attention maps since they own lower head dimensions, and one can apply a linear layer to the attention maps to learn more accurate ones. Along this research line, Zhou et al. (2021b) expand the attention distribution space based on original attention maps without reducing the head dimension, namely *Attention Expansion*. We can observe both *Talking-Head* (Shazeer et al., 2020) and *Refiner* (Zhou et al., 2021b) can maintain the performance when the number of heads is large. However, their gains from more heads are still relatively modest.

In this work, we root the main cause into the following two aspects: 1) the more attention maps generated by *Attention Expansion* own high similarity, which deteriorates the quality of information contained in attention maps. 2) the usage of these heads is coarse, which can not resist the useless information and fully leverage the useful one. To this end, we propose an Enhanced Interactive Transformer, namely EIT, to solve the aforementioned weakness simultaneously. Concretely, we break the vanilla one-to-one mapping and instead adopt a *many-to-many* mapping strategy to acquire more distinct attention maps without sacrificing head dimension. Moreover, we further develop a two-stage enhanced interactive approach to make full use of the diverse subspace information.

Our proposed EIT has been demonstrated to be simple to implement and highly parameter efficient, yet it consistently produces impressive results across a diverse set of tasks including machine translation, grammar error correction, abstractive summarization, language modeling, and brain disease diagnosis. In addition, we have developed a computationally efficient variant of EIT which, while still maintaining strong performance on several tasks, is better suited for low latency industrial applications. Our analysis shows that adding more heads can be an alternative way to improve the expressiveness of Transformer and is orthogonal to enlarging depth or widening the width.

2 PRELIMINARY

Multi-Head Self-Attention in Transformer Multi-head self-attention (MHSA) is an efficient operation that can capture the interactions among tokens. Given an embedded input sequence $\mathbf{X} \in \mathbb{R}^{T \times d}$, MHSA is defined as follows:

$$\mathbf{A}^i = \frac{(\mathbf{X}\mathbf{W}_Q^i)(\mathbf{X}\mathbf{W}_K^i)^\top}{d_k} \quad (1)$$

$$\mathbf{O} = \sum_{i=1}^M \mathbf{A}^i \mathbf{X}\mathbf{W}_V^i \mathbf{W}_O^i \quad (2)$$

where T denotes the sequence length, d is the input embedding dimension, d_k is the head dimension, M is the number of head partition on representations, $\mathbf{W}_Q^i, \mathbf{W}_K^i, \mathbf{W}_O^i \in \mathbb{R}^{d \times d_k}$, $\mathbf{W}_V^i \in \mathbb{R}^{d_k \times d}$. \mathbf{A}^i represents the attention distribution of i -th head. Without special declaration, we use $\mathbf{Q}^i, \mathbf{K}^i, \mathbf{V}^i$ to refer to $\mathbf{X}\mathbf{W}_Q^i, \mathbf{X}\mathbf{W}_K^i, \mathbf{X}\mathbf{W}_V^i$, respectively, which denotes the query, key and value in i -th head.

MHSA with Numerous Heads Given the high efficiency of multi-head strategy to improve the expressiveness of self-attention, researchers try to enhance Transformer by adding more heads. Typically, there are two ways to obtain more attention maps:

- More Head Partition (Vaswani et al., 2017): decreasing d_k to generate more heads, where $d_k \times M = d$ and M is the number of head partition on representations.
- Attention Expansion (Shazeer et al., 2020; Zhou et al., 2021b): $[\mathbf{A}^1, \mathbf{A}^2, \dots, \mathbf{A}^{M^e}] = E([\mathbf{A}^1, \mathbf{A}^2, \dots, \mathbf{A}^M])$, where M^e is the number of heads after *attention expansion* and $E(\cdot)$ is the expansion function which can be linear transformation or convolution.

To use these expanded heads, one often adopts a liner layer to map them to original number of heads as follows: $[\mathbf{A}^1, \mathbf{A}^2, \dots, \mathbf{A}^M] = R([\mathbf{A}^1, \mathbf{A}^2, \dots, \mathbf{A}^{M^e}])$, where $R(\cdot)$ is the linear transformation.

Several phenomena has also shown the advantages of utilizing more heads on other modality such as images. Previous work (Touvron et al., 2021; Zhou et al., 2021c) often equip more heads to improve the expressive of vision Transformer, though their number of heads and gains are still limited.

3 ENABLING TRANSFORMER TO BENEFIT FROM MORE HEADS

In this section, we first analyze the difficulties of benefiting from more heads (Section 3.1). Then we give a detailed description of our proposed EIT that can benefit from more heads efficiently (Section 3.2). Finally, we provide an efficient EIT that removes redundant computation (Section 3.3).

3.1 WHAT ARE THE DIFFICULTIES?

The research aims to examine the effectiveness of the attention maps generated by the attention expansion operation (as described in Section 2) in the context of training 6L-6L pre-norm Refiner and Talking-head models on the WMT’14 En-De task. The head similarity among the attention maps of these models was visualized and measured using cosine similarity (as described in the Appendix B) in Figure 2. Experimental results indicate a high level of redundancy in these numerous attention maps, with an average similarity of nearly 0.50. This redundancy is detrimental to the ability of Talking-head and Refiner to effectively utilize more heads, as the attention maps do not contain sufficient useful information though the number of them is large. Additionally, the utilization of these attention maps is limited by the simple linear transformation method employed by Talking-head and Refiner, which is insufficient to effectively extract useful information from the expanded attention maps, including noisy edges. As such, there is a need for a variant of the multi-head self-attention (MHSA) method that can universally benefit from increased numbers of heads, especially in the case of numerous heads. This will be the focus of the subsequent section.

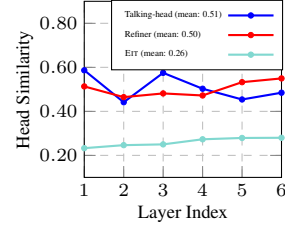


Figure 2: Comparison of head similarity among different heads after attention expansion and many-to-many mapping. We adopt cosine similarity to compute the similarity (the lower the better).

3.2 ENHANCED INTERACTIVE TRANSFORMER

We design a novel Enhanced Interactive Transformer (EIT) in which we replace the multi-head self-attention with Enhanced Multi-Head Attention mechanism (EMHA) that can efficiently benefit from a large number of heads to solve the aforementioned two difficulties.

3.2.1 MANY-TO-MANY MAPPING SCHEME

To efficiently generate a large number of diverse attention maps, we propose a novel many-to-many (M2M) mapping scheme that enable each query to attend to M keys instead of single head. Our motivation lies in the fact that applying dot-multiplication to features is a good way to generate the attention maps¹. As a result, we want to make full use of these partitioned features, e.g., Queries and Keys in Figure 3. As illustrated in Figure 3, four queries and four keys can be served as two components in a bipartite graph and each element in a component, e.g., Q^1 , can interact with any elements in another component, e.g., K^1, \dots, K^4 . Formally, supposing one with M heads, the i -th attention map can be formally calculated as:

$$S^i = \frac{Q^{[(i-1)/M+1]} (K^{(i-1)\%M+1})^T}{\sqrt{d_k}} \quad \forall i \in \{1, \dots, M^2\} \quad (3)$$

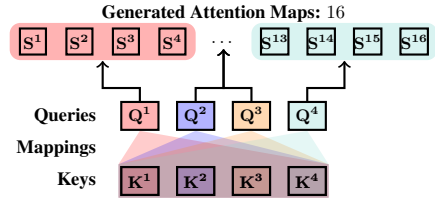


Figure 3: The illustration of many-to-many mapping scheme ($M = 4$).

¹On the one hand, we argue that when the head dimension is sufficient, e.g., larger than 64, such a way to generate attention maps is good. On the other hand, we visualize the similarity among attention maps generated by Transformer with the different number of heads on the En-De task and find that they change little.

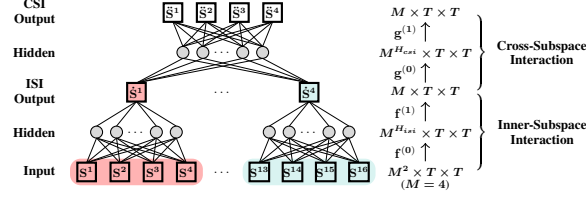


Figure 4: Illustration of dual enhanced interaction in EIT ($M = 4$). We omit the ReLU for simplicity.

where $\mathbf{S}^i \in \mathbb{R}^{T \times T}$ is the attention maps without softmax, $\lfloor \cdot \rfloor$ is the round down operation and $\%$ is the mod operation. For example, \mathbf{S}^4 is computed by \mathbf{Q}^1 and \mathbf{K}^4 when M equals to 4.

Finally, the obtained attention maps are numerous which is the M times of that generated in standard MHSA. These sufficient and diverse attention maps are the key to further benefit from more heads.

3.2.2 DUAL ENHANCED INTERACTION

To better utilize the diverse and numerous attention maps, we design a finer solution that is able to differentiate between relevant and irrelevant information, discarding the latter while fully capitalizing on the former. Two kinds of interactions among those attention maps are introduced hierarchically, the inner-subspace interaction and cross-subspace interaction. The details are as follows:

Inner-Subspace Interaction Relationship As illustrated in Figure 3, the inner-subspace interaction (ISI) relationship describes the connection among the attention maps generated by the same query, e.g., attention maps in the block of same color. These attention maps own a closer relationship. The ISI relationship facilitates the identification and exclusion of non-essential information by allowing for the aggregation of similar data points into more representative clusters from a clustering perspective. This enables the segregation of useful information from insignificant elements.

Inner-Subspace Interaction Modeling One can adopt the standard convolution operation via batch transformation. However, such a way ignores the difference among the ISI relationship constrained by different queries, e.g., the ISI relationship in red block and blue block in Figure 3. It is desirable to preserve and enhance this distinction. To more efficiently model the interaction within subspaces, we therefore adopt group convolutions (Krizhevsky et al., 2012), which use separate parameters to process features from different groups.

Denote $\mathbf{f}(\cdot)$ as a single layer group convolution. As illustrated in Figure 4, given the output of M2M, namely \mathbf{S} , as input, ISI sub-module is computed as:

$$\dot{\mathbf{S}} = \mathbf{f}^{(1)}(\text{ReLU}(\mathbf{f}^{(0)}(\mathbf{S}))) \quad (4)$$

where $\dot{\mathbf{S}} \in \mathbb{R}^{M \times T \times T}$ is the output of the ISI sub-module. We use $M^{H_{isi}}$ to represent the intermediate head size in ISI sub-module and set the number of groups in group convolutions to M .

Finally, we can obtain M high-quality attention maps that effectively retain the benefits of using a larger number of attention heads while discarding irrelevant information. Such a process is another key for Transformer to benefit from more heads and is unique to our work.

Cross-Subspace Interaction Relationship The cross-subspace interaction (CSI) relationship describes the collaboration among different heads. As illustrated in Figure 3, it exists in the attention maps generated by different queries, e.g., attention maps from blocks of different color. Such a relationship provides a suitable solution to fully leverage the information learnt by different heads.

Cross-Subspace Interaction Modeling To efficiently model the cross-subspace interaction, we adopt two-layer convolutions accompanied by the ReLU activation to consist this sub-module.

Let us denote $\mathbf{g}(\cdot)$ as a single layer convolution. As illustrated in Figure 4, given the output of ISI, namely $\dot{\mathbf{S}}$, as input, CSI sub-module is computed as:

$$\ddot{\mathbf{S}} = \mathbf{g}^{(1)}(\text{ReLU}(\mathbf{g}^{(0)}(\dot{\mathbf{S}}))) \quad (5)$$

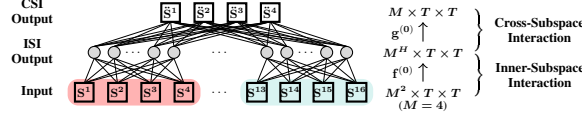


Figure 5: Illustration of dual enhanced interaction in efficient EIT ($M = 4$). We omit the ReLU for simplicity.

where $\ddot{\mathbf{S}} \in \mathbb{R}^{M \times T \times T}$ is the output of the CSI sub-module. We use $M^{H_{csi}}$ to represent the intermediate head size in CSI sub-module. Finally, we can obtain M final attention maps that fully leverage the benefits of each head.

3.3 EFFICIENT VERSION OF EIT

Despite the theoretically computational efficiency and parametric efficiency of group convolutions, they slow down the training in practice (Ma et al., 2018). To alleviate this issue, we provide another efficient version of EIT, namely E-EIT, by simplifying the design of dual enhanced interaction. As illustrated in Figure 5, both ISI and CSI adopt a single-layer operation. Formally, the dual enhanced interactions are computed as:

$$\ddot{\mathbf{S}} = \mathbf{g}^{(0)}(\mathbf{ReLU}(\mathbf{f}^{(0)}(\mathbf{S}))), \quad (6)$$

where $\mathbf{ReLU}(\mathbf{f}^{(0)}(\mathbf{S}))$, namely as $\dot{\mathbf{S}} \in \mathbb{R}^{M^H \times T \times T}$ and $\ddot{\mathbf{S}} \in \mathbb{R}^{M \times T \times T}$ and M^H is a hyper-parameter, e.g. we set it as 32 for the base configuration. In this way, E-EIT avoids parts of memory consumption and somehow improves the computational efficiency.

4 EXPERIMENTS

This section aims to answer following research questions:

- Can EIT stably show superiority to other related work (Section 4.1)?
- Can EIT served as a general backbone on a wide range of applications within and beyond language tasks (Section 4.1-4.5)?
- Where does the improvements of EIT come from (Section 4.6-4.7) and how it reflects on the attention maps (Section 4.8)?

4.1 RESULTS ON MACHINE TRANSLATION

We first examine the effectiveness of EIT on machine translation tasks, an important application in natural language processing. We select two widely used corpus: WMT’14 English-German (En-De) translations (a large-scale dataset) and WMT’16 English-Romanian (En-Ro) translations (a small-scale dataset). The En-De corpus consists of 4.5M training sentence-pairs (source-target). We perform a joint byte-pair encoding (BPE) operation with a size of 32K on all training data. The validation and test sets are *newstest2013* and *newstest2014*, respectively. For the En-Ro task, it consists of 610K training sentence pairs. The preprocessing follows the setups in Mehta et al. (2021). We also perform a joint BPE operation with a size of 20K on the training data.

We build our EIT variants of different configurations ranging over *base*, *big* and *deep* for both tasks. For the En-De task, we select baselines from three aspects: head modification (Zhou et al., 2021b; Shazeer et al., 2020; Wang & Tu, 2020; Li et al., 2019; 2018; Zhang et al., 2022; Nguyen et al., 2022), localness modelling (Li et al., 2022; Fan et al., 2021; Yang et al., 2019), and deep transformer (Liu et al., 2020a; Wang et al., 2019; Wei et al., 2020). A similar selection of baselines is also for the En-Ro task. For a fair comparison, we re-implement some of these models in our codebase, and keep the training setups of these methods the same as ours. We both report BLEU and sacreBLEU² as the evaluation. More details about the experimental setup are included in Appendix A.

Results Table 1 and Table 2 display the results of baselines and our methods on En-De and En-Ro tasks. Through the broad comparison, we can get the following observations:

²BLEU+case.mixed+numrefs.1+smooth.exp+ tok.13a+version.2.0.0

Table 1: BLEU and sacreBLEU points on WMT En-De Task. More details about the settings of these models are given in Appendix C.

Type	Model	WMT'14 En-De		
		θ (M)	BLEU	sBLEU
Head Modification	Refiner (2021b)	-	27.62	-
	Talking-Head (2020)	-	27.51	-
	Collaboration (2020)	-	27.55	-
	DYROUTING (2019)	297M	28.96	-
	DISAGREE (2018)	-	29.28	-
	MoA (2022)	200M	29.40	-
	FISHformer (2022)	-	29.57	-
Localness	DMAN (2021)	211M	28.97	27.8
	CSAN (2019)	-	28.74	-
	UMST (2022)	242M	29.75	-
Deep Transformer	DLCL (2019)	-	29.30	-
	ADMIN (2020a)	262M	30.10	-
	MSC (2020)	272M	30.19	-
Our	Transformer base	62M	27.13	26.0
	EIT base	62M	28.00	26.9
	E-EIT base	62M	27.72	26.7
System (Pre-Norm)	Transformer deep-48	194M	29.60	28.5
	EIT deep-48	194M	30.25	29.2
	E-EIT deep-48	194M	30.16	29.1
	Transformer big	211M	28.80	27.7
	EIT big	212M	29.79	28.7
	E-EIT big	211M	29.61	28.5

Table 2: BLEU points on WMT En-Ro Task. More details about the settings of these models are given in Appendix C.

Type	Model	WMT'16 En-Ro	
		θ (M)	BLEU
Basic Baseline	ConvS2S (2017)	-	29.90
	Transformer (2020b)	-	34.30
	Transformer (2020)	-	34.16
	FlowSeq(2019)	-	31.97
	Int-TF (2021)	-	32.60
	DELIGHT (2021)	53M	34.70
Head modification	Refiner (2021b)	54M	34.25
	Talking-Head (2020)	54M	34.35
	Collaboration (2020)	54M	34.64
	FISHformer (2022)	49M	34.42
	MoA (Zhang et al., 2022)	56M	34.39
Localness	DMAN (Fan et al., 2021)	-	34.49
	UMST (Li et al., 2022)	60M	34.81
Our	Transformer base	54M	34.23
	EIT base	54M	35.10
	E-EIT base	54M	35.01
System (Pre-Norm)	Transformer deep-24	111M	35.00
	EIT deep-24	111M	35.40
	E-EIT deep-24	111M	35.35
	Transformer big	196M	34.44
	EIT big	196M	34.91
	E-EIT big	196M	34.67

1. Our EIT variants outperform the vanilla Transformer with negligible added parameters against different configurations on both datasets. Notably, E-EIT, an alternative to satisfy the low-latency of industrial application, can deliver competitive results compared with the full version with less computations (we show the comparison in Appendix D).

2. Our EIT can beat all selected methods of head modification and localness modelling, including the latest methods such as MoA (Zhang et al., 2022), Fishformer (Nguyen et al., 2022), UMST (Li et al., 2022), on both datasets.

3. Our EIT can beat all selected deep transformers on the En-De task. For example, a 48-layer EIT can beat the 48-layer baseline over 0.69 BLEU points. Besides, compared to MSC and ADMIN, EIT surpasses them with fewer parameters.

All these observations indicate that our EIT variants have stronger expressiveness (Observation 1, 2 and 3). Besides, our modification on head is more effective compared to selected methods (Observation 2). Another thing worth noting is that to decrease the added computation, we only apply the modifications to encoder side. Given this, their influence on inference speed is negligible. More experiments, efficiency analysis and trade-offs strategies are given in Appendix D and E.

4.2 RESULTS ON GRAMMAR ERROR CORRELATION

We also examine the effectiveness of EIT on grammar error correction task, an important application in natural language processing. We conduct experiments on CONLL dataset, which consists of 827K training sentences. We replicate the setup in (Chollampatt & Ng, 2018) and adopt the word-level dropout technique (Sennrich et al., 2016) to alleviate the overfitting problem. We choose the Transformer (Vaswani et al., 2017) and SURFACE (Liu et al., 2021) as the comparisons. All architectures follow the Transformer-base configuration in Vaswani et al. (2017). More details are presented in Appendix A.

Results We exhibit the Precision, Recall, $F_{0.5}$ (most important metrics in this task, higher is better) of different models in Table 3. We can see that both EIT and E-EIT can outperform the standard Transformer by a large margin in terms of $F_{0.5}$, e.g., 0.87 and 1.13 im-

Table 3: Results on the correction task.

Model	Precision	Recall	$F_{0.5}$
Transformer ‡	64.84	36.61	56.18
SURFACE (Liu et al., 2021)	66.80	35.00	56.60
EIT	69.98	32.80	57.05
E-EIT	69.85	33.36	57.31

provements, respectively. They can also show significant superiority compared to SURFACE. Note that both our EIT and E-EIT consume negligible added parameters, e.g., less than 0.1M parameters. So we can conclude that the both EIT and E-EIT have more powerful expressiveness.

4.3 RESULTS ON ABSTRACTIVE SUMMARIZATION

We also test the effectiveness of EIT on abstractive summarization task, a task relying on the ability of modeling long dependency. We select a widely used corpus: CNN/DailyMail dataset which consists of 287K training documents. We perform shared BPE operations with a size of 30K on all the training data. Our models are all under base configuration, e.g., embedding dimension, hidden dimension, M are set to 512, 2048 and 8, respectively. The detailed architecture setups, training setups and evaluation setups are presented in Appendix A.

Results Table 4 shows RG-1, RG-2 and RG-L of different models. We can see both EIT and E-EIT can outperform the standard Transformer by a large margin with scores of 41.62 ROUGE-1 points, 18.70 ROUGE-2 points and 38.33 ROUGE-L points. Compared with other strong baselines, our EIT and E-EIT can still show superiority on these datasets in terms of ROUGE-1 points, e.g., EIT surpasses SURFACE, DMAN and BOTTOM-UP by 0.62, 0.64 and 0.40 in terms of ROUGE-1 points, respectively.

Table 4: Results on the summarization task.

Model	RG-1	RG-2	RG-L
Transformer \ddagger	40.84	18.00	37.58
PG-Net (See et al., 2017)	39.53	17.28	36.38
MADY (Wang et al., 2021)	40.72	17.90	37.21
DMAN (Fan et al., 2021)	40.98	18.29	37.88
BOTTOM-UP (Gehrmann et al., 2018)	41.22	18.68	38.34
SURFACE (Liu et al., 2021)	41.00	18.30	37.90
EIT	41.62	18.70	38.33
E-EIT	41.58	18.63	38.28

Table 5: Comparison of test Perplexity on WikiText-103.

Model	Test PPL
Transformer (Baevski & Auli, 2019)	21.11
EIT	20.00
E-EIT	20.19

Table 6: AUROC, ACC, SEN and SPE points on ABIDE task.

Model	AUROC	ACC	SEN	SPE
MvS-GCN (Wen et al., 2022)	69.0	69.4	69.3	64.5
BrainNetTF (Kan et al., 2022)	80.9 \pm 2.6	71.8 \pm 3.0	71.1 \pm 4.1	72.5 \pm 1.9
BrainNetEITF	81.3 \pm 2.7	73.8 \pm 3.2	73.9\pm5.8	75.6 \pm 4.7
BrainNetE-EITF	82.9\pm3.3	74.6\pm3.2	72.2\pm5.3	76.8\pm3.0

4.4 RESULTS ON LANGUAGE MODELING

We also evaluate our EIT on a language modeling task: WikiText-103 to further examine its ability of modelling long-dependency. The training, validation and test sets consist of 103M words (from 28K articles), 218K words and 246K words, respectively. We follow the official preprocessing procedure (Ott et al., 2019), and select Adaptive Input Transformer (Baevski & Auli, 2019) as the baseline. Both the baseline and our EIT are all 8-layer big models with 8 heads. More details about architecture/training/evaluation setups are given in Appendix A.

Results Table 5 displays the perplexity scores of different models on the test set. We can see that our EIT and E-EIT can outperform the baseline with 1.11 and 0.92 in terms of PPL on the test set, respectively. Given the negligible increased parameters of our methods, we can conclude that the improvements attribute to their high expressiveness.

4.5 RESULTS ON AUTOMATIC BRAIN DISEASE DIAGNOSIS TASK

We further inspect the potential of EIT to be severed as a general method beyond language tasks. The automatic brain disease diagnosis, a disease classification task that highly relies on precisely learning relationships among different brain regions has recently been dominated by graph convolution (Wen et al., 2022) and Transformer (Kan et al., 2022). We select a widely used real-world fMRI dataset: Autism Brain Imaging Data Exchange (ABIDE), which consists of 1009 brain networks from 17 international sites, of which 516 samples are autism spectrum disorder patients. We follow the preprocessing setup in Kan et al. (2022) and adopt the CC200 (Craddock et al., 2012) as the Region-of-Interest (ROI) partition template. We select two latest methods, the Mvs-GCN (Wen et al., 2022) and BrainNetTF (Kan et al., 2022), as our comparison. The experimental setups and configurations of our BrainNetEITF and BrainNetEEITF are the same as in Kan et al. (2022). Each experiment is conducted 5 times and we report the mean and standard deviation of the four metrics: Accuracy (ACC), AUROC, Sensitivity (SEN) and Specificity (SPE).

Results We exhibit the ACC, AUROC, SEN and SPE of different models in Table 6. We can see that both BrainNetEITF and BrainNetEEITF can outperform all the baselines in terms of all metrics. Similarly, thanks to little increased parameters of our models, we can conclude that they have stronger expressiveness and can be easily extended to other scenarios.

4.6 WHERE HIGH EXPRESSIVENESS COMES FROM

High expressiveness does not come from local biases Local modeling is one of the widely accepted ways to improve the expressiveness of Transformer (Yang et al., 2019; Fan et al., 2021; Li et al., 2022). In dual enhanced interaction, we apply convolution operations to attention maps, which has the potential to introduce local biases. To figure it out, we measure the localness of attention maps since if there is a local bias, each token will distribute larger attention weights on their neighboring tokens. We adopt the localness metric of Fan et al. (2021), denoted as \mathcal{C} (higher is better). More details are presented in Appendix.

We plot the \mathcal{C} value within a local region $w = 0.1 * T + 1$, of models in En-De task and CNN-DailyMail task in Figure 6. The value is computed over the test set. Due to the long sequence length, we only use a subset of the test set consisting of 1000 samples for the CNN-DailyMail task. The results (mean) show no significant local enhancement phenomena in both tasks. Note that the attention maps in the first layer of EIT on the abstractive summarization have a strong local pattern, but the kernel sizes are set to 1 on this task. So we conclude that the improvements do not come from local enhancement.

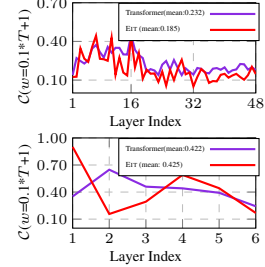


Figure 6: Quantitative analysis on localness in attention maps on En-De task (Above) and CNN-DailyMail task (Bottom).

High expressiveness comes from adding more heads

The feature is always the primary metric to measure the expressiveness of models. Token representation uniformity, also known as oversmoothing, is one of the problems that heavily degrades the capacity of Transformer, especially deep Transformer (Gong et al., 2021; Dong et al., 2021; Shi et al., 2022; Wang et al., 2022). To measure the oversmoothing rate, we define a metric, namely token correlation \mathcal{TC} (the lower, the better). The token correlation is computed by the pearson correlation coefficient (Benesty et al., 2009). More details are given in Appendix F.

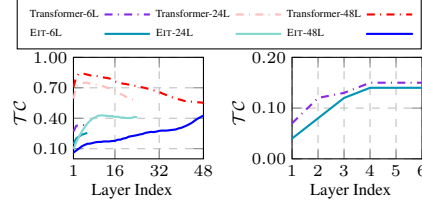


Figure 7: Token correlation of Transformer and EIT on En-De task (left) and CNN-DailyMail task (right).

Figure 7 plots the token correlation of models on the En-De and CNN-DailyMail tasks. We can see that the features learnt by EIT have a lower token correlation than that of vanilla Transformer on both tasks. This indicates EIT has a stronger learning capacity. Moreover, given that adding more heads is theoretically beneficial for anti-oversmoothing (Wang et al., 2022), so the high expressiveness of EIT can be attributed to its use of additional heads. More analyses are given in Appendix F.

4.7 ABLATION STUDIES

Table 7 summarizes the impacts of removing each module on En-De and En-Ro tasks, respectively. First, we find removing any module (or sub-module) mostly results in obvious performance degradation (#3,4,5 v.s #2). Notably, when removing the M2M module (#2 vs. #3), we observe an obvious decline in performance on two translation tasks, which indicates that the importance of M2M module, as it can generate plentiful diverse attention maps. Besides, there is a vast drop in BLEU when removing the ISI sub-module (#2 vs. #4). This is because more heads leads to the existence of some useless information. However, the ISI sub-module provides a suitable way to abandon it while retaining the benefits of the former. This unique design differs from the attention expansion (Zhou et al., 2021b).

Table 7: Ablation study on two tasks. Time denotes the training computing time.

#	M2M	ISI	CSI	En-De		En-Ro	
				BLEU	Time	BLEU	Time
1				27.13	-	34.23	-
2	✓	✓	✓	28.00	1.45×	35.10	1.38×
3		✓	✓	27.39	1.15×	34.71	1.10×
4	✓		✓	25.79	1.22×	32.50	1.21×
5	✓	✓		27.70	1.40×	34.53	1.29×
6	✓			26.01	1.06×	30.67	1.05×
7		✓		27.32	1.30×	34.53	1.25×
8			✓	27.29	1.10×	34.55	1.06×

Moreover, applying a single module (#6, 7, 8 v.s #1, 2) is inferior to EIT, which indicates EIT is well-designed. Note that the additional primary cost comes from the ISI sub-module and partly attributes to the unfriendly support for the implementation of group convolution in PyTorch (Paszke et al., 2019).

4.8 VISUALIZATION OF ATTENTION MAPS

We further reveal how the improvements reflect on the attention maps. We visualize the head similarity among the final attention maps of different models on En-De task in Figure 8. We can see that the attention maps obtained by EIT own higher head similarity compared to other selected models. Different from normal redundant attention maps, the high similarity is the result of benefiting from more heads and fully interactions among different heads. Moreover, these high-similarity attention maps have a property: they are more confident in their decisions (see Appendix G). When we explicitly break this kind of high similarity via regularization in Li et al. (2018), the performance suffers from degradation (from 28.00 to 27.65 under the base configuration).

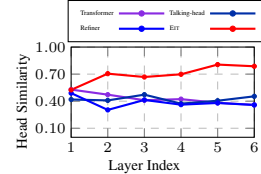


Figure 8: Similarity among attention maps of different models on En-De task.

To further investigate what the high-similarity attention maps can provide, we adopt simple head mask mechanism to prune the heads during inference as follows:

$\mathbf{O} = \sum_{i=1}^M \eta_i \mathbf{A}^i \mathbf{X} \mathbf{W}_V^i \mathbf{W}_O^i$, where $\eta_i \in \{0, 1\}$. We exhibit the BLEU scores of Transformer and EIT on En-De tasks after pruning in Table 8. Note that the selection of

heads are violent, e.g., selecting with index, without considering the importance of heads (Michel et al., 2019), and we only apply the head pruning operations to the encoder side. It is evident that EIT exhibits a high tolerance for head pruning without experiencing significant deterioration in performance. Such phenomenon sheds light on the researches of head pruning and inference speeding.

Table 8: BLEU points of models with head pruning on the En-De task.

Model	Pruning Ratio		
	0.0%	50.0%	87.5%
Transformer-48L	29.60	27.64	1.86
EIT-48L	30.25	29.09	21.12

5 RELATED WORK

Improved Multi-Head Mechanism How to effectively improve the multi-head attention has always been a hot research topic in recent years. Previous work has revealed that multi-head attention can be further enhanced by encouraging individual attention heads to extract distinct information (Li et al., 2018; Cui et al., 2019; Sukhbaatar et al., 2019; Guo et al., 2020; Hao et al., 2019). Another branch of research is designing more complex interactive modeling to make better use of the multiple subspace information (Shazeer et al., 2020; Wang & Tu, 2020; Li et al., 2019). Besides, Voita et al. (2019) empirically demonstrates that some heads in attention are useless and can be pruned without performance degradation. Along this line, researchers investigate how to efficiently cut off redundant heads (Michel et al., 2019; Behnke & Heafield, 2020). Different from these work, Wang et al. (2022) theoretically demonstrates the benefits of multi-head attention. Motivated by it, our work investigates how to benefit from enlarged heads efficiently.

Convolution + Attention Convolution and attention mechanism have been dominated paradigms for local modelling and global modelling, respectively. Collaboration of convolution and attention mechanism has become an interesting topic. Recently, many researchers have shifted their attention to incorporating the convolution into the transformer (Yang et al., 2019; Zhou et al., 2021b; Zhao et al., 2019; Pan et al., 2021; Wu et al., 2021; Xiao et al., 2021; Peng et al., 2021). Their core idea is to fully leverages the advantages of these two paradigms. Our work follows this thread of research but is quite different from them in two aspects: 1) We mainly adopt the convolutions and group convolutions for flexibly modelling the cross-head interaction but not for injecting localness. 2) The convolution of our work is directly applied to the attention map. Note that Zhou et al. (2021b) is similar to our work. However, they mainly focus on modelling the localness bias.

6 CONCLUSIONS

In this paper, we propose EIT, an alternative to the standard multi-head attention network. It further advances the multi-head schema by breaking the standard one-to-one mapping constraint. Meanwhile, EIT employs the inner-subspace interaction and cross-subspace interaction to make full use of the expanded attention maps. In addition, E-EIT can be served as another choice considering the trade-off between performance and computation efficiency. Experimental results on five widely-used tasks demonstrate the effectiveness of EIT-variants, which deliver consistent improvements to the standard Transformer.

REFERENCES

- Alexei Baevski and Michael Auli. Adaptive input representations for neural language modeling. In *International Conference on Learning Representations*, 2019.
- Maximiliana Behnke and Kenneth Heafield. Losing heads in the lottery: Pruning transformer attention in neural machine translation. In *Proc. of EMNLP*, 2020.
- Jacob Benesty, Jingdong Chen, Yiteng Huang, and Israel Cohen. *Pearson Correlation Coefficient*. Springer Berlin Heidelberg, 2009.
- Tom B. Brown, Benjamin Mann, Nick Ryder, Melanie Subbiah, Jared Kaplan, Prafulla Dhariwal, Arvind Neelakantan, Pranav Shyam, Girish Sastry, Amanda Askell, Sandhini Agarwal, Ariel Herbert-Voss, Gretchen Krueger, Tom Henighan, Rewon Child, Aditya Ramesh, Daniel M. Ziegler, Jeffrey Wu, Clemens Winter, Christopher Hesse, Mark Chen, Eric Sigler, Mateusz Litwin, Scott Gray, Benjamin Chess, Jack Clark, Christopher Berner, Sam McCandlish, Alec Radford, Ilya Sutskever, and Dario Amodei. Language models are few-shot learners. In *Proc. of NeurIPS*, 2020.
- Shamil Chollampatt and Hwee Tou Ng. A multilayer convolutional encoder-decoder neural network for grammatical error correction. In *Proc. of AAAI*, 2018.
- R Cameron Craddock, G Andrew James, Paul E Holtzheimer III, Xiaoping P Hu, and Helen S Mayberg. A whole brain fmri atlas generated via spatially constrained spectral clustering. *Human brain mapping*, 2012.
- Hongyi Cui, Shohei Iida, Po-Hsuan Hung, Takehito Utsuro, and Masaaki Nagata. Mixed multi-head self-attention for neural machine translation. In *Proceedings of the 3rd Workshop on Neural Generation and Translation*, 2019.
- Jacob Devlin, Ming-Wei Chang, Kenton Lee, and Kristina Toutanova. BERT: Pre-training of deep bidirectional transformers for language understanding. In *Proc. of NAACL*, 2019.
- Yihe Dong, Jean-Baptiste Cordonnier, and Andreas Loukas. Attention is not all you need: pure attention loses rank doubly exponentially with depth. In *Proc. of ICML*, 2021.
- Zhihao Fan, Yeyun Gong, Dayiheng Liu, Zhongyu Wei, Siyuan Wang, Jian Jiao, Nan Duan, Ruofei Zhang, and Xuanjing Huang. Mask attention networks: Rethinking and strengthen transformer. In *Proc. of NAACL*, 2021.
- Jonas Gehring, Michael Auli, David Grangier, Denis Yarats, and Yann N Dauphin. Convolutional sequence to sequence learning. In *International conference on machine learning*, 2017.
- Sebastian Gehrmann, Yuntian Deng, and Alexander Rush. Bottom-up abstractive summarization. In *Proc. of EMNLP*, 2018.
- Chengyue Gong, Dilin Wang, Meng Li, Vikas Chandra, and Qiang Liu. Vision transformers with patch diversification. 2021.
- Qipeng Guo, Xipeng Qiu, Pengfei Liu, Xiangyang Xue, and Zheng Zhang. Multi-scale self-attention for text classification. In *Proc. of AAAI*, 2020.

- Jie Hao, Xing Wang, Shuming Shi, Jinfeng Zhang, and Zhaopeng Tu. Multi-granularity self-attention for neural machine translation. In *Proc. of EMNLP*, 2019.
- Xuan Kan, Wei Dai, Hejie Cui, Zilong Zhang, Ying Guo, and Carl Yang. Brain network transformer. In *Advances in Neural Information Processing Systems*, 2022.
- Jungo Kasai, James Cross, Marjan Ghazvininejad, and Jiatao Gu. Non-autoregressive machine translation with disentangled context transformer. In *International conference on machine learning*, 2020.
- Diederik P. Kingma and Jimmy Ba. Adam: A method for stochastic optimization. In *Proc. of ICLR*, 2015.
- Alex Krizhevsky, Ilya Sutskever, and Geoffrey E. Hinton. Imagenet classification with deep convolutional neural networks. In *Proc. of NeurIPS*, 2012.
- Bei Li, Tong Zheng, Yi Jing, Chengbo Jiao, Tong Xiao, and Jingbo Zhu. Learning multiscale transformer models for sequence generation. In *Proc. of ICML*, 2022.
- Jian Li, Zhaopeng Tu, Baosong Yang, Michael R. Lyu, and Tong Zhang. Multi-head attention with disagreement regularization. In *Proc. of EMNLP*, 2018.
- Jian Li, Baosong Yang, Zi-Yi Dou, Xing Wang, Michael R. Lyu, and Zhaopeng Tu. Information aggregation for multi-head attention with routing-by-agreement. In *Proc. of NAACL*, 2019.
- Ye Lin, Yanyang Li, Tengbo Liu, Tong Xiao, Tongran Liu, and Jingbo Zhu. Towards fully 8-bit integer inference for the transformer model. In *Proc. of IJCAI*, 2021.
- Xiaodong Liu, Kevin Duh, Liyuan Liu, and Jianfeng Gao. Very deep transformers for neural machine translation. *CoRR*, 2020a.
- Xuebo Liu, Longyue Wang, Derek F. Wong, Liang Ding, Lidia S. Chao, and Zhaopeng Tu. Understanding and improving encoder layer fusion in sequence-to-sequence learning. In *Proc. of ICLR*, 2021.
- Yinhan Liu, Jiatao Gu, Naman Goyal, Xian Li, Sergey Edunov, Marjan Ghazvininejad, Mike Lewis, and Luke Zettlemoyer. Multilingual denoising pre-training for neural machine translation. *Transactions of the Association for Computational Linguistics*, 2020b.
- Ningning Ma, Xiangyu Zhang, Hai-Tao Zheng, and Jian Sun. Shufflenet V2: practical guidelines for efficient CNN architecture design. In *Proc. of ECCV*, 2018.
- Xuezhe Ma, Chunting Zhou, Xian Li, Graham Neubig, and Eduard Hovy. FlowSeq: Non-autoregressive conditional sequence generation with generative flow. In *Proceedings of the 2019 Conference on Empirical Methods in Natural Language Processing and the 9th International Joint Conference on Natural Language Processing (EMNLP-IJCNLP)*, 2019.
- Sachin Mehta, Marjan Ghazvininejad, Srinivasan Iyer, Luke Zettlemoyer, and Hannaneh Hajishirzi. Delight: Deep and light-weight transformer. In *Proc. of ICLR*, 2021.
- Paul Michel, Omer Levy, and Graham Neubig. Are sixteen heads really better than one? In *Proc. of NeurIPS*, 2019.
- Tan Minh Nguyen, Tam Minh Nguyen, Hai Ngoc Do, Khai Nguyen, Vishwanath Saragadam, Minh Pham, Nguyen Duy Khuong, Nhat Ho, and Stanley Osher. Improving transformer with an admixture of attention heads. In *Advances in Neural Information Processing Systems*, 2022.
- Myle Ott, Sergey Edunov, Alexei Baevski, Angela Fan, Sam Gross, Nathan Ng, David Grangier, and Michael Auli. fairseq: A fast, extensible toolkit for sequence modeling. In *Proc. of NAACL*, 2019.
- Xuran Pan, Chunjiang Ge, Rui Lu, Shiji Song, Guanfu Chen, Zeyi Huang, and Gao Huang. On the integration of self-attention and convolution. *CoRR*, 2021.

- Adam Paszke, Sam Gross, Francisco Massa, Adam Lerer, James Bradbury, Gregory Chanan, Trevor Killeen, Zeming Lin, Natalia Gimelshein, Luca Antiga, Alban Desmaison, Andreas Kopf, Edward Yang, Zachary DeVito, Martin Raison, Alykhan Tejani, Sasank Chilamkurthy, Benoit Steiner, Lu Fang, Junjie Bai, and Soumith Chintala. Pytorch: An imperative style, high-performance deep learning library. In *Proc. of NeurIPS*. 2019.
- Zhiliang Peng, Wei Huang, Shanzhi Gu, Lingxi Xie, Yaowei Wang, Jianbin Jiao, and Qixiang Ye. Conformer: Local features coupling global representations for visual recognition. In *Proc. of ICCV*, 2021.
- Abigail See, Peter J. Liu, and Christopher D. Manning. Get to the point: Summarization with pointer-generator networks. In *Proc. of ACL*, 2017.
- Rico Sennrich, Barry Haddow, and Alexandra Birch. Edinburgh neural machine translation systems for WMT 16. In *Proceedings of the First Conference on Machine Translation, WMT 2016, colocated with ACL 2016, August 11-12, Berlin, Germany*, 2016.
- Noam Shazeer, Zhenzhong Lan, Youlong Cheng, Nan Ding, and Le Hou. Talking-heads attention. *CoRR*, 2020.
- Han Shi, Jiahui Gao, Hang Xu, Xiaodan Liang, Zhenguo Li, Lingpeng Kong, Stephen M. S. Lee, and James T. Kwok. Revisiting over-smoothing in BERT from the perspective of graph. In *Proc. of ICLR*, 2022.
- Sainbayar Sukhbaatar, Edouard Grave, Piotr Bojanowski, and Armand Joulin. Adaptive attention span in transformers. In *Proc. of ACL*, 2019.
- Hugo Touvron, Matthieu Cord, Alexandre Sablayrolles, Gabriel Synnaeve, and Hervé Jégou. Going deeper with image transformers. In *Proceedings of the IEEE/CVF International Conference on Computer Vision*, 2021.
- Ashish Vaswani, Noam Shazeer, Niki Parmar, Jakob Uszkoreit, Llion Jones, Aidan N. Gomez, Lukasz Kaiser, and Illia Polosukhin. Attention is all you need. In *Proc. of NeurIPS*, 2017.
- Elena Voita, David Talbot, Fedor Moiseev, Rico Sennrich, and Ivan Titov. Analyzing multi-head self-attention: Specialized heads do the heavy lifting, the rest can be pruned. In *Proc. of ACL*, 2019.
- Huadong Wang and Mei Tu. Enhancing attention models via multi-head collaboration. In *International Conference on Asian Language Processing, IALP 2020, Kuala Lumpur, Malaysia, December 4-6, 2020*, 2020.
- Lihan Wang, Min Yang, Chengming Li, Ying Shen, and Ruifeng Xu. Abstractive text summarization with hierarchical multi-scale abstraction modeling and dynamic memory. In *Proc. of SIGIR*, 2021.
- Peihao Wang, Wenqing Zheng, Tianlong Chen, and Zhangyang Wang. Anti-oversmoothing in deep vision transformers via the fourier domain analysis: From theory to practice. In *Proc. of ICLR*, 2022.
- Qiang Wang, Bei Li, Tong Xiao, Jingbo Zhu, Changliang Li, Derek F. Wong, and Lidia S. Chao. Learning deep transformer models for machine translation. In *Proc. of ACL*, 2019.
- Xiangpeng Wei, Heng Yu, Yue Hu, Yue Zhang, Rongxiang Weng, and Weihua Luo. Multiscale collaborative deep models for neural machine translation. In *Proc. of ACL*, 2020.
- Guangqi Wen, Peng Cao, Huiwen Bao, Wenju Yang, Tong Zheng, and Osmar Zaiane. Mvs-gcn: A prior brain structure learning-guided multi-view graph convolution network for autism spectrum disorder diagnosis. *Computers in Biology and Medicine*, 2022.
- Haiping Wu, Bin Xiao, Noel Codella, Mengchen Liu, Xiyang Dai, Lu Yuan, and Lei Zhang. Cvt: Introducing convolutions to vision transformers. In *Proc. of ICCV*, 2021.
- Tete Xiao, Mannat Singh, Eric Mintun, Trevor Darrell, Piotr Dollár, and Ross B. Girshick. Early convolutions help transformers see better. *CoRR*, 2021.

- Baosong Yang, Longyue Wang, Derek F. Wong, Lidia S. Chao, and Zhaopeng Tu. Convolutional self-attention networks. In *Proc. of NAACL*, 2019.
- Xiaofeng Zhang, Yikang Shen, Zeyu Huang, Jie Zhou, Wenge Rong, and Zhang Xiong. Mixture of attention heads: Selecting attention heads per token. *CoRR*, 2022.
- Guangxiang Zhao, Xu Sun, Jingjing Xu, Zhiyuan Zhang, and Liangchen Luo. MUSE: parallel multi-scale attention for sequence to sequence learning. *CoRR*, 2019.
- Daquan Zhou, Bingyi Kang, Xiaojie Jin, Linjie Yang, Xiaochen Lian, Qibin Hou, and Jiashi Feng. Deepvit: Towards deeper vision transformer. *CoRR*, 2021a.
- Daquan Zhou, Yujun Shi, Bingyi Kang, Weihao Yu, Zihang Jiang, Yuan Li, Xiaojie Jin, Qibin Hou, and Jiashi Feng. Refiner: Refining self-attention for vision transformers. *CoRR*, 2021b.
- Jingkai Zhou, Pichao Wang, Fan Wang, Qiong Liu, Hao Li, and Rong Jin. ELSA: enhanced local self-attention for vision transformer. *CoRR*, 2021c.

A DETAILED SETUPS OF EXPERIMENTS

A.1 MACHINE TRANSLATION TASK

Dataset We evaluated our approach on two widely used machine translation datasets: WMT’14 En-De and WMT’16 En-Ro. The En-De dataset contains approximately 4.5M tokenized training sentence pairs. We selected newstest2013 and newstest2014 as the validation and test data, respectively. As for the En-Ro dataset, it consists of 0.6M tokenized training sentence pairs. We performed shared BPE operations on both datasets to overcome the out-of-vocabulary (OOV) problem. Concretely, we set the size of BPE operations to 32K and 20K for En-De and En-Ro datasets, resulting in a shared vocabulary with sizes of 34040 and 19064, respectively.

Model Configuration Our model architectures are based on Transformer (Vaswani et al., 2017). We provided three basic configurations, namely *base*, *deep*, and *big* which follow the configurations in Vaswani et al. (2017). We adopted a pre-normalization strategy (Wang et al., 2019) considering training stability under different configurations. The detailed settings of hyper-parameters are given in Table 10.

Training & Evaluation Our implementations are based on Fairseq (Ott et al., 2019). Our experiments are performed on the GEFORCE RTX 3090 cards. We use 8 GEFORCE RTX 3090 cards to train models for the WMT’14 En-De task. As for the models on the WMT’16 En-Ro task, we train them on 4 GEFORCE RTX 3090 cards. The batch sizes for En-De and En-Ro tasks are 65536 and 16384, respectively. The total updates are 50K, 50K and 100K for *base*, *deep* and *big* in En-De task, respectively. We adopt Adam (Kingma & Ba, 2015) as an optimizer with an adam_β of (0.9, 0.997). The learning rate scheduler is *invert_sqrt* with a learning rate of 0.002 and warmup updates of 16000. We also adopt label smoothing with a ratio of 0.1 in all the experiments. More details are exhibited in Table 11. During the evaluation process, we set the beam number to 4 and the length penalty to 0.6 for the En-De task. As for the En-Ro task, the number of beams is 5 and the length penalty is 1.3.

Table 9: The details of datasets of language tasks.

Dataset	Sentence			BPE	Vocab
	Train	Dev	Test		
WMT’14 En-De	4.5M	3.0K	3.0K	32K	34040
WMT’16 En-Ro	0.6M	2.0K	2.0K	20K	19064
CNN/DailyMail	287K	13.0K	11.0K	30K	32584
CONLL	827K	5.4K	1.3K	30K	33136
WikiText-103	103M	218K	246K	-	267740

A.2 ABSTRACTIVE SUMMARIZATION TASK

Dataset For abstractive summarization, we conduct experiments on a widely used corpus, e.g., CNN/DailyMail dataset. It consists of 287K training documents. Shared BPE operations with a size of 30K are performed on all the training data, resulting in a vocabulary of 32584.

Model Configuration We only provide the *base* configuration of our EIT and E-EIT for abstractive summarization. The details are presented in Table 10.

Training & Evaluation We train models for an abstractive summarization task on 8 GEFORCE RTX 3090 cards with a batch size of 131072 and total updates of 30K. We adopt a weight decay strategy with a ratio of 0.0001. Other hyper-parameters are the same as that in machine translation tasks. You can find their settings in Table 11. During testing, the number of beams is set to 4 and the length penalty is set to 2.0. Besides, we set the minimal length and maximum length to 55 and 140, respectively.

Table 10: The configurations of models on three sequence generation tasks. MT, AS, GEC and LM denote machine translation, abstractive summarization, grammar error correction and language modelling, respectively.

Task	Model	Configuration	M	M ^H	M ^{H_{isi}}	M ^{H_{csi}}	r	K _h ^{isi}	K _w ^{isi}	K _h ^{csi}	K _w ^{csi}
MT	EIT	<i>base</i>	8	-	128	64	8	1	7	1	3
		<i>deep</i>	8	-	128	64	8	1	7	1	3
		<i>big</i>	16	-	256	256	16	1	7	1	3
	E-EIT	<i>base</i>	8	32	-	-	8	1	7	1	7
		<i>deep</i>	8	32	-	-	8	1	7	1	7
		<i>big</i>	16	64	-	-	16	1	7	1	7
AS	EIT	<i>base</i>	8	-	8	64	8	1	1	1	1
	E-EIT	<i>base</i>	8	16	-	-	8	1	1	1	1
GEC	EIT	<i>base</i>	8	-	128	128	8	1	7	1	3
	E-EIT	<i>base</i>	8	64	-	-	8	1	7	1	7
LM	EIT	<i>big</i>	8	-	64	32	8	1	1	1	1
	E-EIT	<i>big</i>	8	8	-	-	8	1	1	1	1

Table 11: The training setups of different tasks. UF denotes the update frequency of the gradient. (.) lists the values of hyper-parameters under the *big* configuration, which vary from the values under the *base* configuration.

Hyper-parameter	WMT’14 En-De	WMT’16 En-Ro	CNN/DailyMail	CONLL	WikiText-103
GPUs	8	4	8	8	8
Batch	4096	4096	4096	4096	1024
UF	2	1	4	2	8
Optimizer	Adam	Adam	Adam	Adam	Nag
Adam _β	(0.9, 0.997)	(0.9, 0.997)	(0.9, 0.997)	(0.9, 0.980)	-
LR	0.0020	0.0020	0.0020	0.0015	0.0001
LR scheduler	inverse sqrt	inverse sqrt	inverse sqrt	inverse sqrt	Cosine(t-mult=2)
Initial LR	1e ⁻⁷	1e ⁻⁷	1e ⁻⁷	1e ⁻⁷	1e ⁻⁷
Total updates	50K (100K)	25K	30K	14K	286K
Warmup updates	16000	8000	8000	4000	16000
Weight decay	0.0000	0.0000	0.0001	0.0001	0.0000
Label smoothing	0.1	0.1	0.1	0.1	0.0
Dropout	0.1 (0.3)	0.1 (0.3)	0.1	0.2	0.3
Attention dropout	0.1	0.1	0.1	0.1	0.1
ReLU dropout	0.1	0.1	0.1	0.1	0.1
Word dropout	0.0	0.0	0.0	0.2	0.1

A.3 GRAMMAR ERROR CORRECTION TASK

Dataset For the grammar error correction task, we select the CONLL dataset to evaluate our approach. The CONLL dataset consists of 827K training sentences. We replicate the setup in Chollampatt & Ng (2018) and adopt the word-level dropout technique (Sennrich et al., 2016) to alleviate the overfitting problem. More details are listed in Table 9.

Model Configuration For grammar error correction task, we only provide the *base* configuration of our EIT and E-EIT. The details are presented in Table 10. Notice that the models on this task adopt a post-normalization strategy.

Training & Evaluation We train models for the grammar error correction task on 8 GEFORCE RTX 3090 cards. The batch size is 65536 and the total updates are 14K. More training details are shown in Table 11. During testing, the beams and length penalty are set to 6 and 0.6, respectively.

A.4 AUTOMATIC DISEASE DIAGNOSIS TASK

Dataset For the automatic disease diagnosis task, we select the ABIDE dataset to evaluate our approach. The ABIDE dataset consists of 1009 brain networks from 1009 real samples of 17 international sites. Due to the heterogeneity of this data, we adopt the shared data with re-standardized data splitting in Kan et al. (2022). Specifically, 70%, 10% and 20% samples are served as the training, validation and test sets, respectively.

Model Configuration For ABIDE task, we still follow the model configuration in Kan et al. (2022). Specifically, we build our BrainNetEITF with two-layer encoder. The number of heads M are set to 4 for each layer.

Training & Evaluation We train all models including the BrainNetTF and BrainNetEITF from 200 epochs on a single GEFORCE RTX 3090 card. Each model is trained by 5 times. We adopt Adam (Kingma & Ba, 2015) as an optimizer with an initial learning rate of 10^{-4} and a weight decay of 10^{-4} . The batch size is set to 64. We adopt the checkpoint of the final epoch for evaluating the test set.

A.5 LANGUAGE MODELING TASK

Dataset For the language modeling task, we select the WikiText-103 dataset to evaluate our approach. The training set consists of 103M words from 28K articles. While for the validation and test sets, they are made up of 218K and 246K words, respectively. In details, we follow the instructions in Fairseq (Ott et al., 2019) to obtain and preprocess the data. The details are listed in Table 9.

Model Configuration For WikiText-103 task, Both baseline and our model are all 8-layer big model with 8 heads. Note that the baseline we adopted are adaptive input transformer (Baevski & Auli, 2019). In this task, the kernel sizes in DEI are all set to 1.

Training & Evaluation The training and evaluation settings all follow the standard instructions for language modeling in PyTorch (Ott et al., 2019). We train both baseline and EIT with 286000 updates. The details are given in Table 11. As for the evaluation process, we adopt the checkpoint performing best on the validation set. We set the max-tokens, max-sentences, context-window to 3072, 1 and 2560, respectively.

B DETAILS OF METRICS

B.1 CALCULATION OF HEAD DISTANCE

Inspired by the attention metrics in Zhou et al. (2021a) and Wang et al. (2022), we measure the distance between different heads by calculating cosine similarity among attention maps. Notice that our metric focuses on the diversity of attention maps, which is quite different from them. Denote the dataset as \mathcal{D} , and the attention map of h -th head of l -th layer of i -th sample denotes as $\mathbf{A}^{(h,l,i)}$, the head similarity in l -th layer is computed by averaging the cosine similarity of every two heads in i -th layer across all samples as:

$$\mathcal{H}\mathcal{D}^{(l)} = \frac{1}{|\mathcal{D}|} \frac{1}{M(M-1)} \frac{1}{T} \sum_{i=1}^{|\mathcal{D}|} \left(\sum_{j=1}^M \sum_{k=1}^M \sum_{t=1}^T \frac{|\mathbf{A}_{t,:}^{(j,l,i)} \mathbf{A}_{t,:}^{(k,l,i)}|}{\|\mathbf{A}_{t,:}^{(j,l,i)}\|_2 \|\mathbf{A}_{t,:}^{(k,l,i)}\|_2} - M \right) \quad (7)$$

where $|\mathcal{D}|$ denotes the size of dataset, M is the number of partition of features in attention and T is the sequence length. We set \mathcal{D} to the test set of the corresponding task. The obtained head similarity ranges from $[0, 1]$. The larger the head similarity, the lower the distances between different heads are.

B.2 CALCULATION OF TOKEN CORRELATION

We define a metric \mathcal{TC} , which measures the correlation among the representations of different tokens. Denote the dataset as \mathcal{D} , and the sequence representation of i -th sample in l -th layer denotes as $\mathbf{X}^{(l,i)}$, the token correlation of in l -th layer is computed as:

$$\mathcal{TC}^{(l)} = \frac{1}{|\mathcal{D}|} \frac{1}{T(T-1)} \sum_{i=1}^{|\mathcal{D}|} \left(\sum_{j=1}^T \sum_{k=1}^T \frac{\sum_{s=1}^d (\mathbf{X}_{j,s} - \bar{\mathbf{X}}_{j,\cdot})(\mathbf{X}_{k,s} - \bar{\mathbf{X}}_{k,\cdot})}{\sqrt{\sum_{s=1}^d (\mathbf{X}_{j,s} - \bar{\mathbf{X}}_{j,\cdot})^2 \sum_{s=1}^d (\mathbf{X}_{k,s} - \bar{\mathbf{X}}_{k,\cdot})^2}} - T \right) \quad (8)$$

where $\bar{\cdot}$ is the mean operation. Intuitively, the larger the \mathcal{TC} is, the higher the token correlation is, degrading the model’s learning capacity (Gong et al., 2021).

C DETAILED ADDED PARAMETERS OF OUR METHODS

Table 12: Detailed parameters of models on WMT En-De and WMT En-Ro tasks.

Model	En-De			En-Ro		
	Base	Deep-48L	Big	Base	Deep-24L	Big
Transformer	61.56 M	193.96 M	211.22 M	53.90 M	110.64 M	195.88 M
EIT	61.63 M	194.32 M	211.55 M	53.98 M	111.09 M	196.40 M
E-EIT	61.57 M	194.14 M	211.30 M	53.92 M	110.73 M	195.97 M

Table 13: Detailed parameters of models on CNN-DailyMail, CONLL, WikiText-103 and ABIDE tasks.

Model	CNN-DailyMail	CONLL	WikiText-103	ABIDE
Transformer	60.82 M	61.10 M	146.49 M	3.98 M
EIT	60.83 M	61.19 M	146.50 M	3.98 M
E-EIT	60.82 M	61.15 M	146.49 M	3.98 M

The detailed parameters of models on all tasks are listed in Table 12 and Table 13. We can see that the increased parameters are negligible on all tasks. Thus, we can exclude the effect of increasing parameters on performance.

D MORE ANALYSIS ON THE EN-DE TASK

D.1 ANALYSIS ON PLACEMENT OF DEI

Table 14 compares the impacts on several placements of DEI module, e.g., ISI \rightarrow Softmax \rightarrow CSI. First, Softmax operation is insensitive to the placement of the CSI sub-module, which results in negligible BLEU degradation (#1 vs. #2). Moreover, by comparing #2 and #3, we find that when placing the ISI sub-module behind the Softmax, the performance suffers a obvious BLEU drop on both tasks compared to EIT. This indicates that design of EIT is optimal.

Table 14: Effect on placement of DEI on two tasks. Here, IB and IA denote the ISI module is located *before* or *after* the Softmax function, and so on for CSI.

#	IB	IA	CB	CA	En-De	En-Ro
1	✓		✓		28.00	35.10
2	✓			✓	27.93	34.88
3		✓		✓	27.50	34.45

D.2 EFFECT OF COLLABORATION

CSI modeling explicitly enhances the collaboration among different heads. Intuitively, such an enhancement of collaboration enables each head to contain information from other heads. To validate this, we design an experiment as follows:

- We follow the calculation in Eq. (4), Eq. (5) and Eq. (6) to obtain the attention maps.

- we select one attention maps as a shared one across all heads as follows: $\mathbf{O} = \sum_{i=1}^M \mathbf{A}^1 \mathbf{X} \mathbf{W}_V^i \mathbf{W}_O^i$.

We conduct experiments on models under base configuration on both En-De and En-Ro tasks. The training of these models are the same as that given in Appendix A.

We exhibit the results in Table 15. We find that both EIT and E-EIT with selected attention map are still superior to the standard Transformer on two translation tasks. This indicates that the information contained in one head of EMHA is comparable to that in eight heads of standard MHSA.

Table 15: Ablation study on the collaboration of different heads.

#	Model	En-De	En-Ro
1	Transformer	27.13	34.23
2	EIT (selected attn)	27.20	34.72
3	E-EIT (selected attn)	27.17	34.65

D.3 EFFECT OF THE NUMBER OF ORIGINAL FEATURES SUBSPACES PARTITION M

In our EIT, the size of M directly influences the number of attention maps we can obtain, e.g., M^2 attention maps. To investigate its effect on performance, we conduct experiments with different M on the En-De task. The results are exhibited in Figure 9. We can see that the performance gap between EIT and Transformer increases as the M grows. This indicates that EIT has good ability of utilizing these attention maps. For example, when M is 16, EIT achieves BLEU scores of 28.06 on the En-De task.

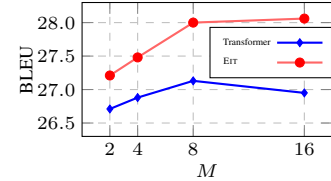


Figure 9: BLEU vs. the size of M on the En-De task.

D.4 EFFECT OF ENCODER DEPTH

As analysed in Section 4.6, EIT can learn more powerful representations with lower token correlation, which has been proved to be beneficial for deep Transformers. To validate this, we exhibit the performance of EIT with different encoder depths on the En-De task in Figure 10. We can see EIT is well scalable to deep configurations. For example, EIT outperforms the Transformer at all depths with up to 0.69 BLEU points on average. Similar phenomena could be observed in E-EIT. Notably, EIT-48L and E-EIT-48L can achieve BLEU points of 30.25 and 30.16 with consumption of only 194M parameters, respectively.

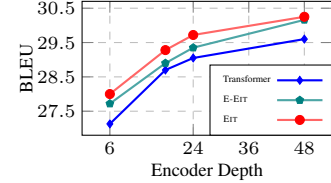


Figure 10: BLEU vs. encoder depth on the En-De task.

D.5 EFFICIENCY COMPARISON

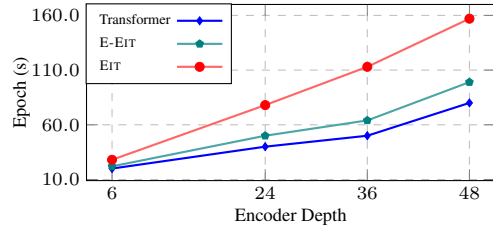
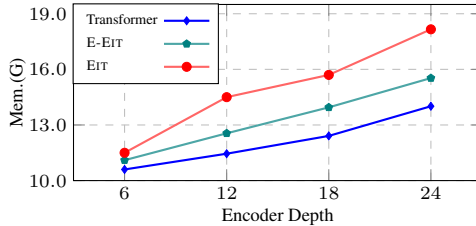


Figure 11: Memory and speed vs. encoder depth. E-EIT can achieve comparable results with fewer training costs than EIT.

Despite the performance evaluation, the memory consumption and computational cost are also two major concerns in the literature. Figure 11 also displays the memory consumption and computational cost of models on the En-De task. EIT only costs 8.5% more memory consumption and 44.4% more training costs than the baseline with a depth of 6. However, the extra consumption goes larger as the depth goes deeper. To make it lighter, we conduct tremendous parameters analysis to provide many guidelines to trade off efficiency and performance (section E).

Besides, as aforementioned, we elaborately design an efficient version E-Eit that only costs 9.4% more memory consumption and 21.7% more training costs than the baseline under all the config-

urations on average. In this work, the many-to-many mapping rule is only applied on the encoder side. This is because the proposed M2M module and the subsequent ISI and CSI sub-modules will significantly enlarge the inference cost due to the heavy use of product attention on the decoder side, although it can attain further benefits in terms of BLEU.

D.6 VISUALIZATION OF TRAINING AND VALIDATION PERPLEXITY

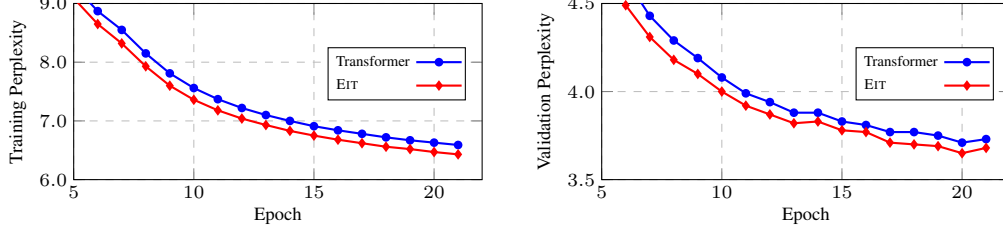


Figure 12: Training perplexity and validation perplexity of Transformer and our EIT on WMT’14 En-De task. Note that the models are in *base* configuration.

We plot the training and validation perplexity of Transformer and our EIT on the WMT’14 task in Figure 12. We can see that our EIT owns lower training and validation perplexity than Transformer.

E EFFICIENCY/PERFORMANCE TRADE-OFFS (CASE OF EN-DE MACHINE TRANSLATION)

E.1 MANY-TO-MANY MAPPING WITH ANY SIZE OF RECEPTIVE FIELD

In some cases, there is no need to adopt the many-to-many mapping scheme in which each query can attend to all keys. We call the regions that each query can attention as *receptive field*. Given this requirement, We provide a general design of many-to-many mapping method with any size of receptive field. We give a general definition of receptive field with any size r as follows: $\Psi(\mathbf{Q}^i, r) = \{\mathbf{K}^k | k = (i + j - 1) \% M, j = 1, 2, \dots, r\}$. Through this definition, we construct EIT with different receptive field. We exhibit the BLEU points of them on the En-De task in Figure 13. We can see that EIT with all choice of receptive field can consistently outperform Transformer. Notably, when the size of receptive field is 2, the performance gap between EIT and Transformer is significant.

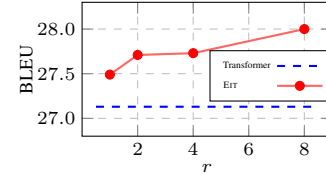


Figure 13: BLEU vs. the size of receptive field on the En-De task.

E.2 NUMBER OF EIT ENCODER LAYERS

We further dig out the effect of the number of EIT encoder layers on the performance. This can also be served as a way to trade-off between computational efficiency and performance. Figure 14 exhibited the results. We can see our EIT can maintain a high-level performance even when the number of EIT layers is one. The reason is that, as illustrated in Figure7, the standard Transformer has a higher token correlation even in the first layer, which does harm to the learning of later layers, while our EIT in the shallow layers can maintain a low-level token correlation. Thus, they can collaborate well.

Motivated by this phenomenon, we further apply such design to the big configuration. We set the number of layers as 2, and keep the training strategy the same as that in Appendix A. Surprisingly, We can train a big model with a performance of 29.29 within 7.12 hours, which cut off 31% training costs while improving 1.7% performance.

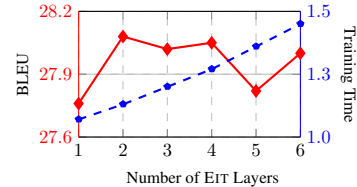


Figure 14: Efficiency/Performance trade-offs against the number of EIT layers.

E.3 OTHER EFFICIENCY/PERFORMANCE TRADE-OFFS (KERNEL SIZE AND HIDDEN SIZE)

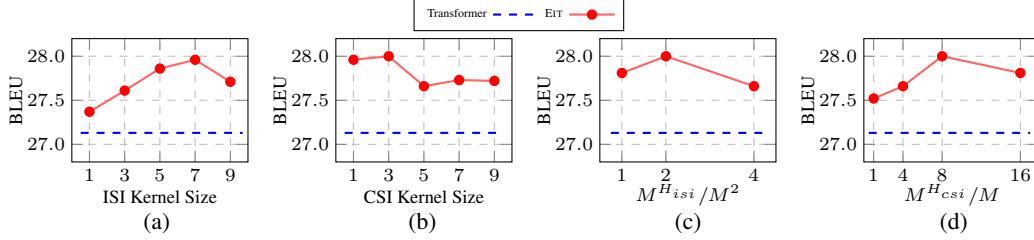


Figure 15: The comparison of BLEU against different hyper-parameters. Note that the blue horizontal line represents the performance of Transformer.

Since there are several hyper-parameters in both ISI and CSI sub-modules, it is necessary to figure out how they affect performance. Figure 15 (a-d) plots the performance of EIT against the kernel size and the hidden size. We can see that EIT can outperform Transformer in all choice of kernel size and hidden size. This observation can further help us trade off efficiency and performance well. For example, we can set csi kernel size to 1 or isi kernel size to 3 or $M^{H_{isi}}$ to M^2 or $M^{H_{csi}}$ to $4M$ to own a more efficient EIT.

F MORE DISCUSSION ABOUT OVERSMOOTHING AND FEATURES COLLAPSE (THE CASE OF EN-DE MACHINE TRANSLATION)

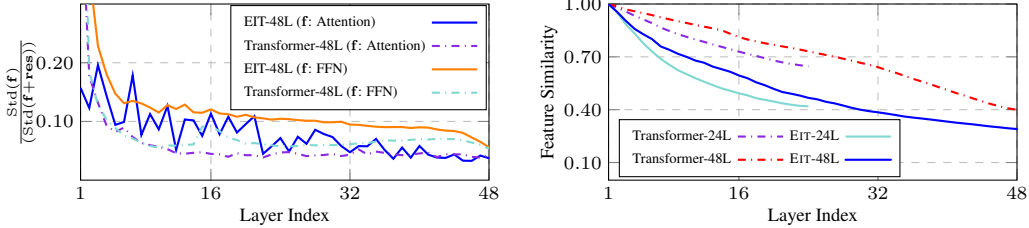


Figure 16: Quantitative analysis on feature similarity across layers. The features similarity is measured by the similarity between features of each layer and the features of first layer. We adopt the cosine similarity to measure the similarity (Zhou et al., 2021a).

As analysed in Section 4.6, EIT has the property of anti-oversmoothing. To further investigate it, we define a metric, namely \mathcal{UR} , to measure the utilization ratio of functions. Given a function f , its utilization ratio $\mathcal{UR}(f)$ is calculated as follows:

$$\mathcal{UR}(f) = \frac{\text{std}(f)}{\text{std}(f + \text{res})} \quad (9)$$

where $\text{std}(f)$ denotes the standard deviation of the output of function f and $\text{std}(f + \text{res})$ denotes the standard deviation of the output of function f added the residual.

Figure 16(left) plots the ratio of function output and final output of our EIT and Transformer models on the En-De task. We can see that Attention and FFN in EIT contribute more to the module output. This is unusual since Attention and FFN have a tendency to learn similar token representations and the residual connection is of great benefit to resist this tendency (Dong et al., 2021; Wang et al., 2022). Such a phenomenon also indicates that Attention and FFN in EIT has a tendency to learn lower similar token representation than those in Transformer. So they do not rely too much on the residual connection.

We further connect it with features collapse, another important problem in deep learning. Intuitively, higher utilization ratio of functions in Transformer can help model learn more distinct representations. To validate this, we plot the cross-layer similarity of features of models on the En-De task in Figure 16(right). We follow the metric defined in Zhou et al. (2021a) to calculate the cross-layer similarity of features. We can see that the final representation learnt by EIT encoder is more distinct from that learnt by the first layer of encoder than Transformer. We hope this phenomenon can shed light on the researches of this line.

G MORE VISUALIZATION (THE CASE OF EN-DE MACHINE TRANSLATION AND CNN-DAILMAIL ABSTRACTIVE SUMMARIZATION)

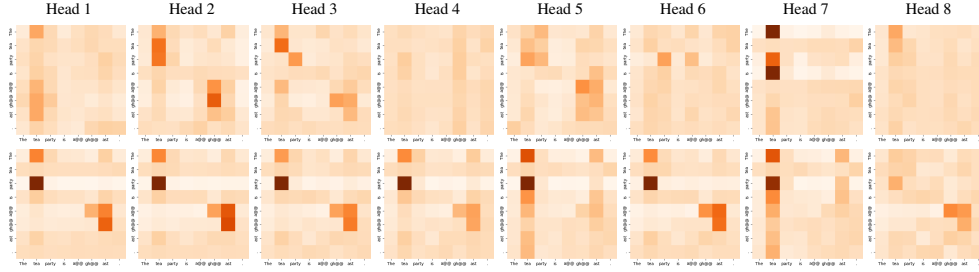
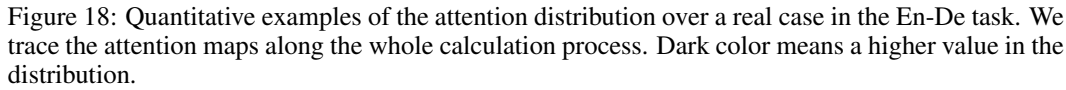


Figure 17: Quantitative examples of the attention distribution over a real case in WMT’14 En-De task. The above is the distribution generated by the standard Transformer, and the below is ours (EIT). Dark color means a higher value in the distribution.

Visualization of Examples in the En-De Task We visualize the attention maps (Figure 17) for an example on the En-De task, and get the following observations: 1) Attention maps obtained by EIT attend to certain patterns, e.g., word boundary information (a@@, gh@@ and ast) (Li et al., 2022). 2) Our attention maps are more confident in their decision, e.g., each token pays more attention to a few positions rather than learning a smoothing view over all positions. These demonstrate that our EIT can generate more precise attention maps. Besides, though the nearly consistent attending results lead to the high similarity among attention maps, we find that if the patterns are useful, high-similarity attention maps are not a drawback.

Detailed Visualizations of Attention Maps in the En-De Task In this section, we visualize attention maps of each period, e.g., M2M, ISI and CSI. The results are exhibited in Figure 18. We can see that M2M can indeed generate a large number of diverse attention maps. We also plot the attention maps generated by *Attention Expansion* in Figure 19. The attention maps generated by *Attention Expansion* own high similarity. Some attention maps even degrade to a nearly uniform distribution, such as the attention map placed in row 1 and column 5. These attention maps may lead to some inefficiency since they seem to be useless.

Visualization of Examples in Abstractive Summarization Task We also plot the attention distributions of a real case in the abstractive summarization task in Figure 20 (Transformer) and Figure 21 (EIT). We can see that the attention maps of all subspaces generated by EIT have a strong weight within the diagonal region. As for Transformer, only a few attention maps can capture such information.



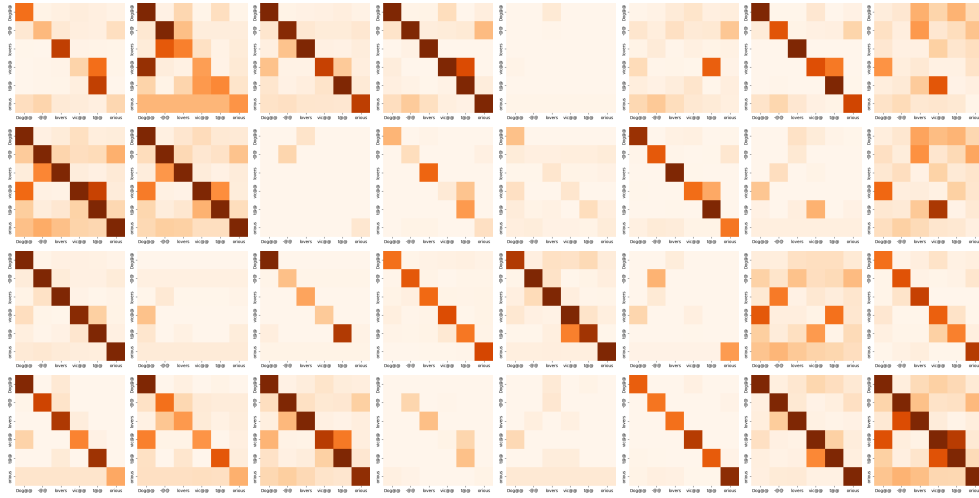


Figure 19: Quantitative examples of the attention distribution obtained by *Refiner* over a real case in the En-De task. Dark color means a higher value in the distribution. Note that we select the best setup (32) for *Refiner* to visualize.

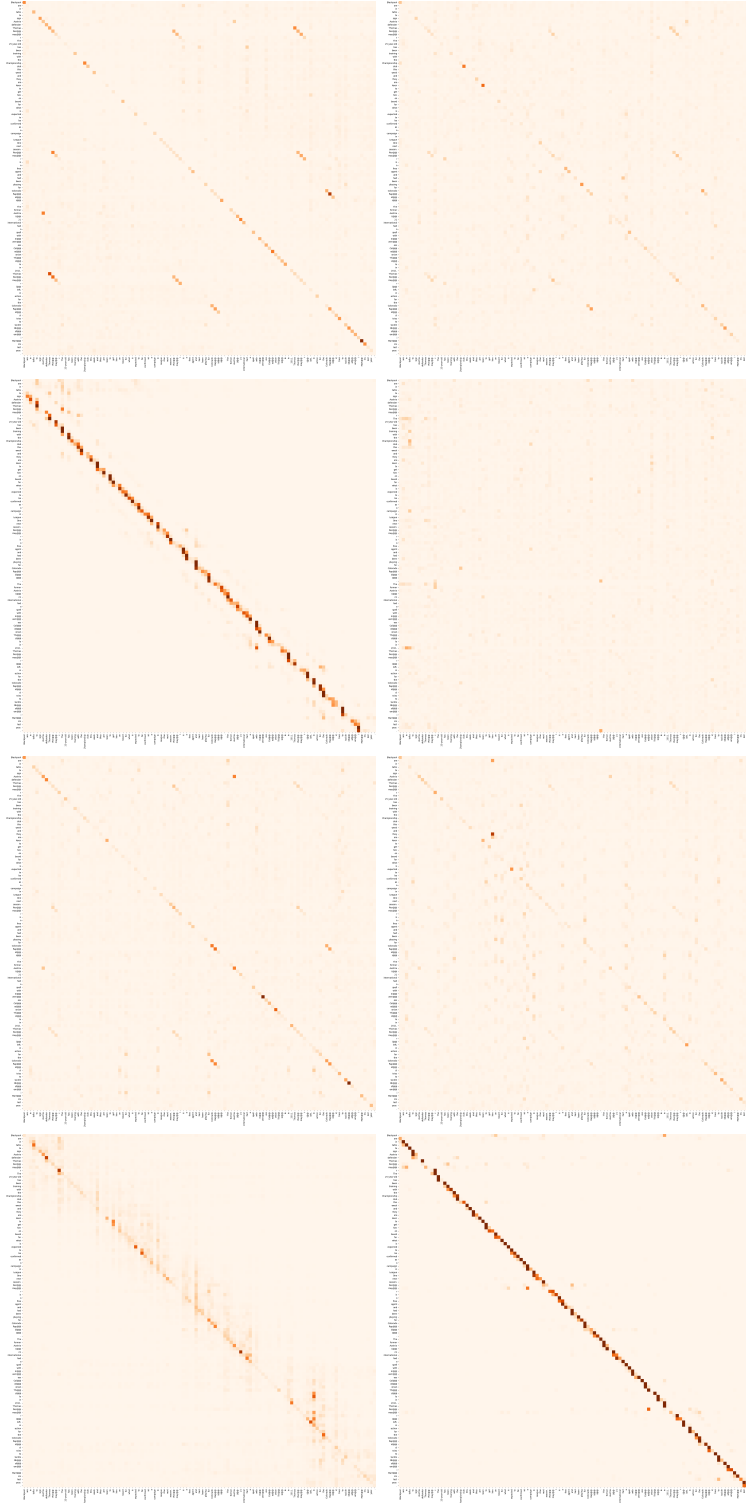


Figure 20: Quantitative examples of the attention distribution over a real case in the abstractive summarization task. The attention maps come from eight subspaces of Transformer. Dark color means a higher value in the distribution.

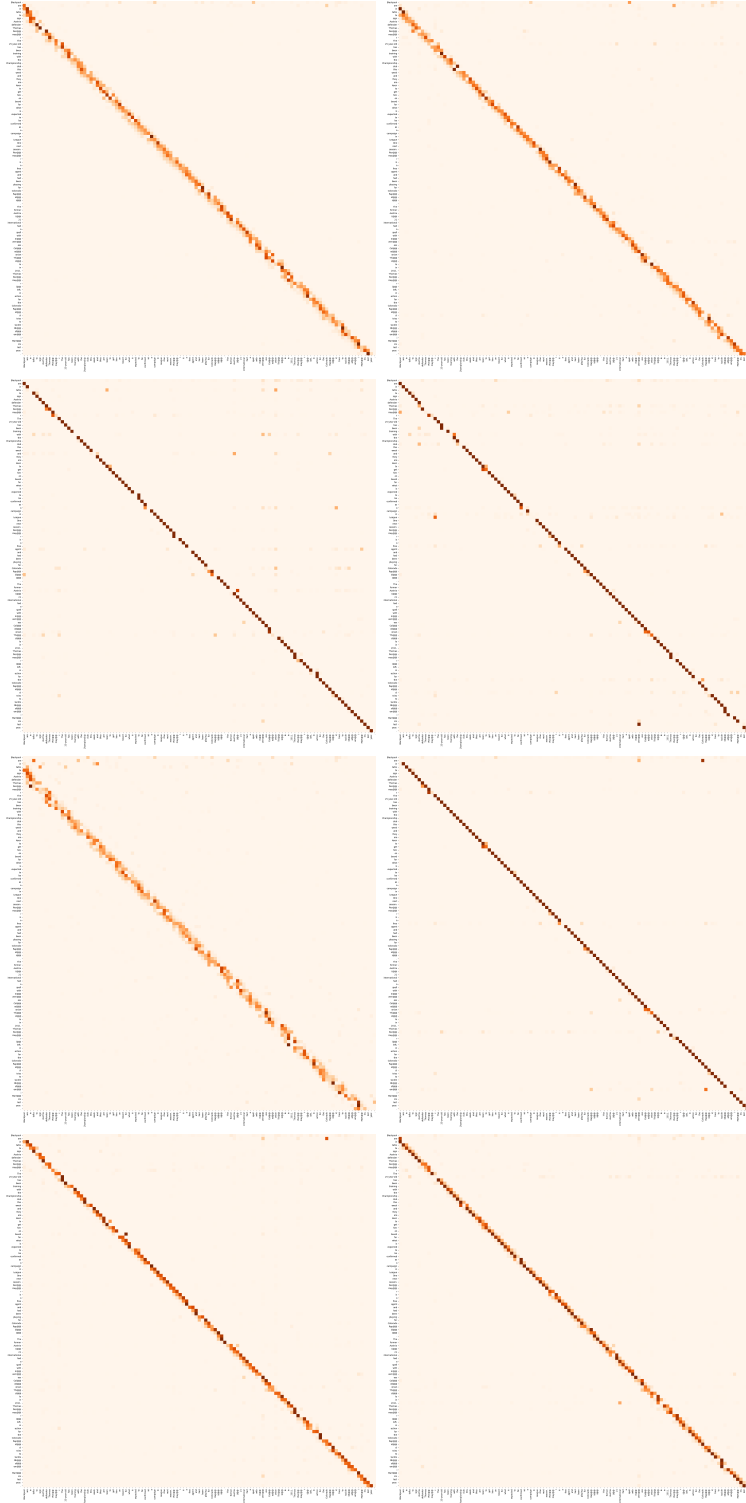


Figure 21: Quantitative examples of the attention distribution over a real case in the abstractive summarization task. The attention maps come from eight subspaces of EIT. Dark color means a higher value in the distribution.